Active Control of the Strong Coupling Regime between Porphyrin Excitons and Surface Plasmon Polaritons

Audrey Berrier,[†,*] Ruud Cools,[†] Christophe Arnold,[†] Peter Offermans,[‡] Mercedes Crego-Calama,[‡] Sywert H. Brongersma,[‡] and Jaime Gómez-Rivas[†,§]

[†]Centre for Nanophotonics, FOM Institute AMOLF c/o Philips Research Laboratories, High Tech Campus 4, 5656 AE Eindhoven, The Netherlands, [‡]Holst Centre/Imec-nl, High Tech Campus 31, 5656 AE Eindhoven, The Netherlands, and [§]COBRA Research Institute, Eindhoven University of Technology, P.O. Box 513, 5600 MB Eindhoven, The Netherlands

ABSTRACT We experimentally demonstrate the active control of the coupling strength between porphyrin dyes and surface plasmon polaritons supported by a thin gold layer. This control is externally exerted by a gas flow and is reversible. The hybridized exciton–polariton branches resulting from the exciton–plasmon coupling display a splitting proportional to the coupling strength of the light–matter interaction. The coupled system changes from the weak (no splitting) to the strong coupling regime (splitting of 130 meV) by controlling the effective oscillator strength in the dye layer, *via* exposure to nitrogen dioxide. The modification of the coupling strength of the system allows tailoring of the dispersion of the hybridized modes as well as of their group velocity.

KEYWORDS: normal mode coupling · polariton splitting · porphyrin dye · surface plasmon polariton · strong coupling · active control

Understanding and controlling light–matter interactions is a major objective of photonics. In particular, the coupling between an emitter and an electromagnetic (EM) mode constantly attracts a wide research interest. This interaction was first studied in atomic physics, where experiments detailed the behavior of atoms in a microwave cavity.[1,2] Later the field expanded to semiconductor physics with confined electrons (quantum well excitons) and confined photons (microcavities).[3−6] The term vacuum Rabi splitting (VRS), referring to the energy splitting of a single atomic transition coupled to a cavity mode, has often been used when the system involves more than a single oscillator, *e.g.*, the case of many atoms or dye molecules or of quantum wells.[7] In the many-oscillator system the behavior is classical; that is, adding one extra oscillator to the system has little effect. It has been shown that the behavior of the system under the latter regime is well described by inserting the complex refractive index of the excitonic medium into the transfer matrix formalism.[8−10] If the absorption linked to the excitonic state is strong and narrow enough compared to the width of the EM mode, two polaritonic branches appear. This case corresponds to normal mode coupling (NMC), sometimes also called many-emitter VRS. The Rabi splitting is proportional to the oscillator strength of the transition,[11] which in the many-oscillator case varies with the square root of the number of excited molecules. Active control of the coupling between excitons and surface plasmon polaritons is of significant interest for a fundamental understanding of light–matter interactions and for applications in nanoplasmonics. Recently ultrafast modification of the excitonic–plasmonic coupling was demonstrated using excitonic nonlinearities.[12]

In this work, we demonstrate a simple method to prepare the hybridized exciton–polariton states at a given coupling strength, from weak to strong. In particular, we present a method to actively control the many-emitter VRS by modifying the strength of the coupling between a porphyrin dye and surface plasmon polaritons. This modification of the coupling strength is controlled by a reaction between a layer of dye molecules and NO_2 gas, which modifies the total oscillator strength of the layer, and depends on the gas concentration. The prepared system is stable at constant gas concentration and can be reversed by heating under nitrogen flow. We show that this characteristic behavior can be used to tailor the normal mode coupling to a surface plasmon polariton as well as actively slow down the polariton. The oscillator strength of Frenkel excitons in organic semiconductors, such as those investigated here, is usually much larger than that of inorganic semiconductors. Therefore the interaction strength of such excitons with EM modes is much larger than their inorganic analogues.

* Address correspondence to a.berrier@amolf.nl.

Received for review March 22, 2011 and accepted July 21, 2011.

Published online July 21, 2011
10.1021/nn201077r

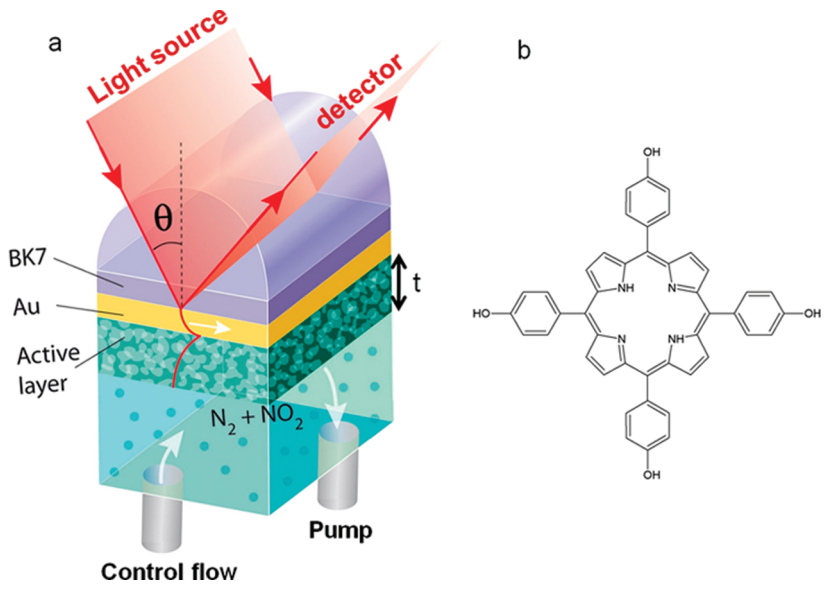

Figure 1. (a) Schematic representation of the experimental setup in the attenuated total reflection (ATR) configuration illustrating the flow cell, the porphyrin silica hybrid nanocomposite (active layer), and the gold layer (50 nm) on the BK7 glass substrate. The excitation of the surface plasmons is realized by the cylindrical prism. (b) Representation of the OH-2H-TPP dye molecule embedded in the active layer.

Moreover, Frenkel excitons are observable at room temperature. A few studies of strong coupling of organic excitons placed in a microcavity used porphyrin[13] or cyanine[12,14] dyes. Porphyrin dyes are known to develop an excitonic peak at 1.77 eV when exposed to NO_2 gas molecules.[15] The interaction of porphyrin molecules with NO_2 molecules has been exploited in gas-sensing schemes.[16] The study of the modifications of the NMC by a modification of the nonlinear saturation of excitons in quantum wells placed in a microcavity has already been proposed as a tool to study the behavior of the inorganic semiconductor excitons.[17]

SURFACE PLASMON POLARITONS

Surface plasmon polaritons (SPPs) are electromagnetic modes propagating at the interface between a metal and a dielectric. These modes are extremely sensitive to changes in the permittivity (or complex refractive index) of the dielectric.[18] The dispersion relation of SPPs propagating at the interface between a metallic layer and an infinitely thick dielectric layer is given by

$$k_{spp} = \frac{\omega}{c}\mathrm{Re}\left\{\sqrt{\frac{\varepsilon_{metal}\varepsilon_{layer}}{\varepsilon_{metal}+\varepsilon_{layer}}}\right\} \quad (1)$$

where k_{spp} is the wavevector of the surface plasmon polariton along the propagation direction, ω is the angular frequency, c is the velocity of light in a vacuum, ε_{metal} is the complex permittivity of the metal layer, and ε_{layer} is the complex permittivity of the dielectric layer. An SPP has a greater wavevector than the corresponding propagating photon at the same frequency in the surrounding dielectric; therefore we cannot couple to the SPP mode by direct illumination. The coupling of free space radiation to SPPs can be achieved by total internal reflection in a high refractive index prism. This coupling takes place when the parallel component of the wavevector of the incident radiation in the prism (with respect to the interface), $(2\pi/\lambda)n_p \sin\theta$, where θ is the angle of incidence and n_p the refractive index of the prism, is equal to k_{spp}. Therefore, for the experiments, the sample is fixed on a half-cylindrical lens acting as a prism using index matching liquid ($n = 1.51$). The sample is mounted on a setup that allows the gas flow and the rotation of the sample and a detector to measure the specular reflection. Figure 1 illustrates the experimental configuration. More details can be found in the Methods section.

RESULTS AND DISCUSSION

Experimental. Figure 2 shows the measurements of the attenuated total reflectance as a function of energy and wavevector for different NO_2 gas concentrations in the control flow. The NO_2 concentration varies between 0 and 6 ppm. The band of low reflectance in Figure 2a corresponds to the coupling of the incident light to SPPs at the interface between the gold and the active layer when the sample is not exposed to the reactive gas. In Figure 2b, c, and d we can see the evolution of the SPP dispersion curve as the gas concentration is increased. The anticrossing behavior between the porphyrin exciton at 1.77 eV and the SPP results in a splitting of the dispersion curve into two polaritonic branches, as seen in Figure 2d. The anticrossing is the signature of the strong coupling regime between the excitons and SPPs with the width of the splitting at the resonance being proportional to the strength of the mode coupling. The observed splitting

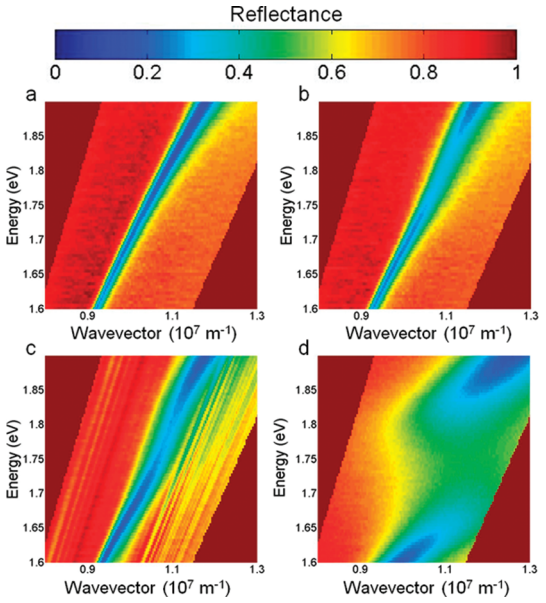

Figure 2. Experimentally obtained dispersion relations of the surface plasmons as a function of the NO_2 gas concentration C in the flow cell under N_2 flow: (a) C = 0 ppm; (b) C = 0.3 ppm; (c) C = 4.6 ppm; (d) C = 6 ppm.

has been given different names in the literature, such as normal mode splitting[17] or surface polariton splitting.[19] We will use the term mode splitting in the following. The magnitude of the mode splitting increases with the number of activated excitonic oscillators per unit volume, N_{act}, itself proportional to the active gas concentration. The effective mode coupling constant G, characterizing the rate at which energy is transferred between the EM mode and matter, varies as $G = gN_{act}^{1/2}$; where $g = S_{mode}f_{osc}$ is the coupling constant between a single oscillator and the EM mode,[2] with S_{mode} the mode strength and f_{osc} the oscillator strength for one oscillator. The strength of the coupling depends on the comparison of G with the rate at which light escapes from the EM mode κ_{EM} and the decay rate of the exciton $\gamma_{osc.}$ Therefore a variation in N_{act} acts directly upon the strength of the mode coupling since it modifies the value of G. The strong coupling regime is usually reached when G becomes larger than both κ_{EM} and γ_{osc}.[20] The control of the number of active gas molecules N_{act} gives us the possibility to switch between a regime of weak coupling, for which light and matter do not interact more strongly inside the coupled system than with the outside of the system, and a regime of strong coupling, for which light and matter exchange energy for a certain number of periods before the energy escapes the system.

Modeling. The optical properties of the layered system can be calculated using the transfer matrix method (TMM), where the dispersion of the exciton is included in the permittivity of the active layer using a linear dispersion model in which the organic excitons are treated as single Lorentz oscillators. In this model the variables are the effective oscillator strength per unit volume, the excitonic line width, and the thickness of the active layer. The spin coating of a solution with a porphyrin concentration of 1.25 g/L results in a final layer of 65 nm after solvent evaporation. The permittivity of the porphyrin layer is given by[10]

$$\varepsilon(\omega) = \varepsilon_b + 9.10^{-20}\frac{F}{(\omega_j^2 - \omega_0^2 - i\gamma\omega)} \qquad (2)$$

where ε_b is the complex permittivity of the background, ω_0 is the angular frequency of the absorption line, γ is the damping of the transition, ω is the angular frequency, and F is the effective oscillator strength density of the active layer. We define the effective oscillator strength density of the active layer as $F = N_{act}f_{osc}$, with f_{osc} the absorption molecular oscillator strength for one molecule and N_{act} the number of activated excitons per unit volume, *i.e.*, $N_{act} = PN_{total}$, with P being the fraction of porphyrin molecules that are activated by NO_2 and N_{total} the density of porphyrin molecules.

It is difficult to estimate the total amount of activated molecules present in the porous layer, as well as the individual molecular oscillator strength. It is well known that the environment influences the oscillator strength. Molecular oscillator strengths have been reported to range from several units for J-aggregates to 10^{-2} for porphyrin dyes in a silica environment.[21] For the modeling of the optical properties of the active layer we use an effective oscillator strength density with an order of magnitude 10^{29} m^{-3}. In our modeling of the permittivity of the active layer we take only the oscillator at 1.77 eV into account. When the magnitude of the splitting is on the order of magnitude of the line width of the resonance, the two peaks are indistinguishable. Figure 3 shows the result of the TMM calculations based on the model described above. Figure 3a displays the variation of n and k (respectively real and imaginary components of the refractive index) of the active layer as the effective oscillator strength density varies from 8×10^{28} to 6×10^{29} m^{-3}. The black curves are the values of n and k experimentally obtained by ellipsometry for an active layer exposed to a NO_2 concentration of 1.3 ppm. The absorbance peak increases with the effective oscillator strength. Figure 3b and c represent an enlargement of the calculated reflectance around the energy of the exciton (1.77 eV). The calculated energy−wavevector reflectance diagrams reproduce the experimental behavior seen in Figure 2.

Group Velocity. The dispersive behavior of the surface plasmon polaritons close to the excitonic mode can be tailored by the control flow of NO_2 molecules. Figure 4a presents the minimum of reflectance, as obtained from the experiments, for different gas concentrations. The group index, defined as $n_g = v_g/c = (1/c)(\partial\omega/\partial k)$, where

v_g is the group velocity, is plotted in Figure 4b. At the wavelength of 560 nm, the value of the group index can be varied from 1.40, when no gas is flowed over the structure, up to 2.80, when a gas concentration of 6 ppm is used. This experimental demonstration of the active control of the polaritonic propagation shows the ability to significantly slow SPPs by modifying the flow of gas. Since the gas–active layer interaction is reversible,[22] it is possible to recover the initial state of the sample after gas exposure, hence controlling the release of the slowed polariton and recovering its initial group velocity.

Mode Splitting. The polaritonic mode splitting increases with the absorbance of the layer. The reflectance curve at a fixed wavevector k has two dips, characteristic of strong mode coupling. The width of the mode splitting Ω is a measure of the strength of the exciton–SPP interaction. It is interesting to look at the evolution of the splitting of the polaritonic modes as a function of the effective oscillator strength of the active layer. Figure 5 shows the cuts of the calculated energy–wavevector diagrams at minimum mode splitting, *i.e.*, zero detuning between the EM mode and the excitonic mode. When the fraction of activated porphyrins (P) increases, the reflectivity minimum becomes less pronounced and the dip of the curves gets flattened out. When the energy width of the splitting is large enough, we can resolve two reflectivity dips (Figure 5a). For such a curve, we can measure the energy separation between the dips, giving a measure for the mode splitting. The evolution from the weak coupling to the strong coupling regime can be achieved by a modification of the mode strength (depending on, for instance, the quality factor of the resonance of the EM mode) or by modification of the properties of the excitonic state, *i.e.*, the effective oscillator strength density F. For small values of P or N_{act} we are in the regime of weak coupling; that is, only one reflectivity peak is visible and its full width at half-maximum (fwhm) increases. If N_{act} is increased further, we reach the point when the eigenenergies of the system split with equal linewidths. From that point on, the fwhm of the modes decreases as we enter the strong coupling regime.[3] In the strong coupling regime, the light–matter interaction is no longer a weak perturbation but becomes a strong perturbation of the energy levels of the active medium. Figure 5b shows that the mode splitting is linear as a function of the square root of the absorbance of the active layer. One notes here that if the splitting is obtained from wavelength–angle reflectance maps, the dependence *versus* the square root of the absorbance would also be linear, but with a larger slope and higher offset. Thus this would give inappropriately larger values for the mode splitting. However, it is possible to use the two linear dependences to "translate" the energy separation of the reflectivity peaks measured from a wavelength–angle plot into the value for normal mode splitting. We will use this procedure to obtain the values of the mode splitting displayed in Figure 6.

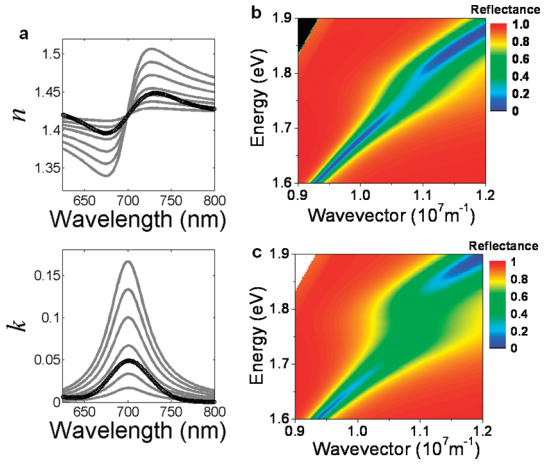

Figure 3. (a) Real (n) and imaginary (k) components of the refractive index of the active layer calculated from a Lorentzian oscillator model with the effective oscillator strength density varying from 0.8×10^{29} to 8×10^{29} m^{-3} (percentage of activated porphyrins, P, varying from 10% to 100%) displayed as gray curves. The black curves correspond to the real and imaginary components of the refractive index of the active layer exposed to a NO_2 concentration of 1.3 ppm. The black curves coincide with the calculated index with $P = 0.3$. (b) Calculated reflectance in an ATR configuration with an effective oscillator strength density of 3.2×10^{29} m^{-3}. (c) Same as (b) with an effective oscillator strength density of 6.4×10^{29} m^{-3}.

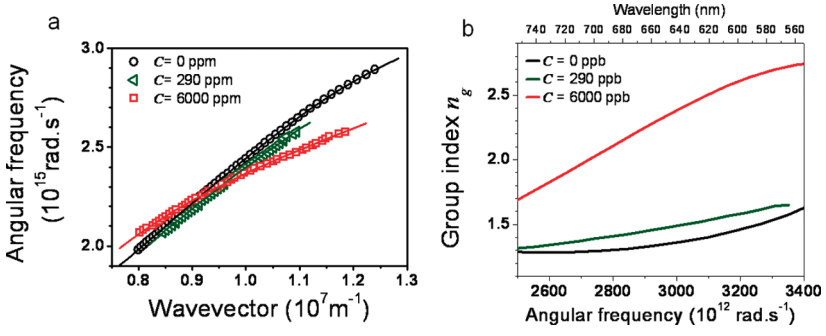

Figure 4. (a) Measured (symbols) dispersion relation of the lower polaritonic branch around 1.77 eV for different concentrations (C) of the active gas. The continuous curves are polynomial fits of the experimental data. (b) Group index extracted from the fits of the polaritonic branches of (a).

From Weak to Strong Coupling. We have demonstrated a direct way to tune the splitting between the polaritonic modes of a coupled system by modification of the effective oscillator strength, F, which can be achieved by changing the number of activate oscillators, N_{act}. The variation of N_{act} is obtained by varying the NO_2 concentration in the control flow and waiting for the equilibrium to settle. It is also possible to take advantage of the diffusion of the gas into the porous layer to get a time-dependent variation of N_{act}. Figure 6a presents the time evolution of the reflectance spectra experimentally obtained at a fixed angle. The broadening of the polaritonic resonance gradually increases, and ultimately the splitting into the two branches occurs. We underline that the angle of incidence, not the wavevector, is kept constant in the experiments. This explains why the reflectance dips of the two polaritonic branches are not identical after splitting. The splitting measured in Figure 6a can be translated into the mode splitting using a corresponding wavelength/angle to energy/wavevector as described earlier. We have fitted the experimental data (fits shown in Figure 6b) using the transfer matrix method in order to obtain the relative variation of the effective oscillator strength density as a function of the strength of the splitting. We note that a slight variation in angle would imbalance the reflectance curves, leading to a higher reflectance at shorter wavelength and lower reflectance at longer wavelengths. This imbalance explains the differences between the experimental and calculated curves at longer wavelengths.

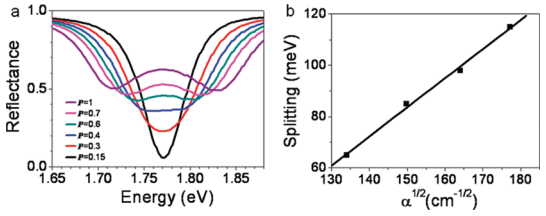

Figure 5. (a) Linecuts of the calculated dispersion maps at the wavevector inducing a surface plasmon resonance at 700 nm (1.77 eV) for an increasing value of the activation percentage P as indicated in the legend. (b) Energy splitting obtained from the energy−wavevector maps as a function of the square root of the absorbance of the layer.

Figure 6c presents the evolution of the full attenuated total reflectance spectra, at a fixed angle of incidence θ, as a function of the exposure time to NO_2. At time $t = 0$ the active gas molecules are introduced in the control flow. The gas molecules diffuse into the active layer and increase the coupling strength G by increasing the number of active oscillators. In the time-resolved reflectance spectra we can see that the fwhm of the reflectivity dip increases from 0 to about 100 s before forming two branches of reduced fwhm as the time, *i.e.*, the number of NO_2 molecules captured by porphyrin molecules, increases. The increase of the fwhm before splitting corresponds to the increase of the radiative losses of the coupled polaritons−exciton mode in the regime of weak coupling.

The time evolution of the mode splitting is shown in Figure 6d. The filled squares after 120 s correspond to the regime of strong coupling, where the separation between the two branches can be measured. At longer

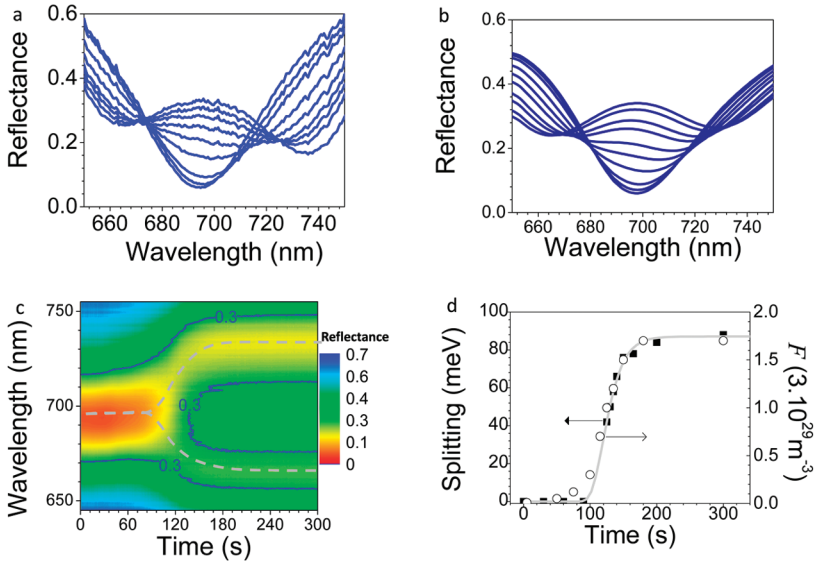

Figure 6. (a) Experimental reflectance spectra obtained at a fixed angle (53°) as a function of time (from 5 to 300 s). The NO_2 concentration is 4.6 ppm. (b) Calculated reflectance spectra obtained with the Lorentzian model, with an effective oscillator strength density varying from 0.03×10^{29} to 5.1×10^{29} m^{-3}. (c) Time-resolved reflectance spectra obtained at a fixed angle (53°) under gas flow with a NO_2 concentration of 4.6 pm. The blue curves are the contour curves of reflectance 0.3. The gray dotted curves are guides to the eye. (d) Time evolution of the energy splitting between the two polariton modes as obtained from experimental data by conversion to an energy−wavevector map (black squares). On the same graph is shown the extracted effective oscillator strength density obtained from the fits to the measurements (open circles).

time the splitting saturates, reaching the equilibrium. On the same graph, the open circles represent the extracted values of the effective oscillator strength density as obtained from the fits to the experimental curves (Figure 6b). This graph relates the mode splitting and the oscillator strength density. The regime of weak coupling occurs for $F < 1.5 \times 10^{29}$ m^{-3}, whereas strong coupling occurs for larger values of F. The saturation value of both the mode splitting and F depends on the concentration of active gas molecules in the flow: a larger mode splitting is obtained for a higher concentration of NO_2 molecules in the control flow. For a NO_2 concentration of 4.6 ppm, the maximum splitting is 90 meV, while for a NO_2 concentration of 6 ppm (Figure 2d) the maximum measured splitting is 130 meV.

Similarly to the increase of the mode splitting presented in Figure 6b, it is possible to decrease the mode splitting by reversing the reaction between NO_2 and the porphyrin molecules. The decrease of the number of oscillators is attainable by heating the sample. A complete reversal of the polaritonic splitting was obtained by heating the sample at 75 °C for a few minutes. After recovery of the initial state, the active layer can still operate in a similar fashion, as shown in Figure 5; that is, it is therefore possible to go back from a normal mode doublet toward a single reflectivity peak, and *vice versa*.

In conclusion, we have experimentally demonstrated the active control of the coupling between excitons of a molecular dye and the surface plasmon polaritons at the interface with a flat gold interface. The sample can be brought from the weak coupling into the strong coupling regime with a polaritonic splitting that can be tuned by acting on the concentration of NO_2 gas reacting with the dye. The magnitude of the mode splitting reaches 130 meV in our experimental range of gas concentrations. Using a model based on the transfer matrix method with Lorentzian oscillators describing the permittivity of the dye, we extract the variation of the effective oscillator strength of the active layer and relate it to the mode splitting. We confirm that the essential physical parameter determining the behavior of the system is the number of activated oscillators. This method paves the way for an active control of the polaritonic branches of coupled hybrid organic–inorganic system and can be applied to tailor the coupling strength of dyes to guided, cavity, localized, and lattice modes.

METHODS

The samples consist of a glass substrate, a 50 nm gold layer, and a 65 nm active layer. The active layer is made of an organic–inorganic hybrid nanocomposite with interconnected nanometer pores (nanoporous silicon oxide) in which the porphyrin molecules are embedded.[23] The porosity of the matrix allows the increase of the thickness of the active layer while keeping an open path for the gas molecules to reach the active sites on the porphyrin molecules. A thicker active layer increases the overlap of the porphyrin molecules with the electromagnetic field profile of the surface plasmon polariton.

The porphyrin family of molecules plays an important role in biology, as it includes hemoglobin, myoglobin, cytochromes, and chlorophyll.[24] They are very versatile molecules, as they can be used as active elements for molecular switches,[25] energy harvesting systems,[26] nonlinear optical materials,[22] and optical gas sensors.[16,27] They are highly conjugated macrocycles known for their high chemical stability and characterized by their distinctive absorption spectrum in the visible due to their electronic structure.[15] The highly conjugated flat ring of the porphyrins gives rise to very intense absorption bands in the UV–vis spectra due to $\pi-\pi^*$ transition and the corresponding vibronic modes. The adsorption of NO_2 perturbs the electronic distribution of the aromatic ring by interacting with carbon atoms of the outer pyrole rings.[28] This interaction induces a new excitonic state in the band gap of the organic semiconductor, giving rise to a characteristic absorption band around 700 nm (1.77 eV), also named the Q-band.[15]

In this work we use 5,10,15,20-tetrakis(4-hydroxyphenyl)-21*H*,23*H*-porphine (2H OHTPP), commercially purchased from Sigma-Aldrich and used without further purification. 2H OHTPP molecules possess the typical crown structure of porphyrins with two substituent phenol groups (Figure 1b). When the active layer is exposed to the NO_2 gas, an extra absorbance peak appears around 1.77 eV, as confirmed by ellipsometry measurements on the exposed active layer. The sample is inserted into a flow cell in which the active layer is in contact with the gas. The control flow (as defined in Figure 1) uses nitrogen (N_2) as a carrier gas and a variable concentration of NO_2 molecules. NO_2 is inserted into the flow cell with different concentrations ranging from 0.3 to 6 ppm. The NO_2 molecules diffuse into the porous matrix of the active layer and react with the porphyrin molecules, hence activating the excitonic oscillators.

For the attenuated total reflectance measurements, light from a halogen lamp impinges from a cylindrical lens onto the gold layer. The reflected light is collected by a spectrometer. The sample is positioned on a two-axis rotational stage where both the angle of incidence (θ) and the angle of detection (specular reflection) can be varied. Since surface plasmons can be excited only by p-polarized light, a polarizer is set in the light path to control the polarization of the incident light. The measurements with s-polarization are used as reference. The specular reflectance spectra are collected as a function of the angle of incidence and subsequently transformed into energy–wavevector diagrams.

Acknowledgment. A.B. would like to thank A. Lagendijk for helpful discussions. This work is part of the research program of the "Stichting voor Fundamenteel Onderzoek der Materie (FOM)", which is financially supported by the "Nederlandse Organisatie voor Wetenschappelijk Onderzoek (NWO)". It is part of the industrial partnership program between Philips and FOM.

REFERENCES AND NOTES

1. Nogues, G.; Rauschenbeutel, A.; Osnaghi, S.; Bruna, M.; Raimond, J.-M.; Haroche, S. Seeing a Single Photon without Destroying It. *Nature* **1999**, *400*, 239–242.
2. Agarwal, G. S. Vacuum-Field Rabi Splittings in a Microwave Absorption by Rydberg Atoms in a Cavity. *Phys. Rev. Lett.* **1984**, *53*, 1732–1734.
3. Weisbuch, C.; Nishioka, M.; Ishikawa, A.; Arakawa, Y. Observation of the Coupled Exciton-Photon Mode Splitting in a Semiconductor Quantum Microcavity. *Phys. Rev. Lett.* **1992**, *69*, 3314–3317.

4. Houdré, R.; Stanley, R. P.; Oesterle, U.; Ilegems, M.; Weisbuch, C. Room Temperature Cavity Polaritons in a Semiconductor Microcavity. *Phys. Rev. B* **1994**, *49*, 16761–16764.
5. Stanley, R. P.; Houdré, R.; Weisbuch, C.; Oesterle, U.; Ilegems, M. Cavity-Polariton Photoluminescence in Semiconductor Microcavities: Experimental Evidence. *Phys. Rev. B* **1996**, *53*, 10995–11007.
6. Agarwal, G. S. Vacuum-field Rabi Oscillations of Atoms in a Cavity. *J. Opt. Soc. Am. B* **1985**, *2*, 480–485.
7. Khitrova, G.; Gibbs, H. M.; Kira, M.; Koch, S. W.; Scherer, A. Vacuum Rabi Splitting in Semiconductors. *Nat. Phys.* **2006**, *2*, 81–90.
8. Zhu, Y.; Gauthier, D. J.; Morin, S. E.; Wu, Q.; Carmichael, H. J.; Mossberg, T. W. Vacuum Rabi Splitting as a Feature of Linear-Dispersion Theory: Analysis and Experimental Observations. *Phys. Rev. Lett.* **1990**, *64*, 2499–2502.
9. Savona, V.; Andreani, L. C.; Schwendimann, P.; Quattropani, A. Quantum Well Excitons in Semiconductor Microcavities: Unified Treatment of Weak and Strong Coupling Regimes. *Solid State Commun.* **1995**, *93*, 733–739.
10. Jackson, J. D. *Classical Electrodynamics*, 3rd ed.; John Wiley & Sons: New York, 1998.
11. Loudon, R. *The Quantum Theory of Light*; Oxford University Press: New York, 2000.
12. Vasa, P.; Pomraenke, R.; Cirmi, G.; De Re, E.; Wang, W.; Schwieger, S.; Leipold, D.; Runge, E.; Cerullo, G.; Lienau, C. Ultrafast Manipulation of Strong Coupling in Metal-Molecular Aggregate Hybrid Nanostructures. *ACS Nano* **2010**, *4*, 7559–7565.
13. Lidzey, D. G.; Bradley, D. D. C.; Skolnick, M. S.; Virgili, T.; Walker, S.; Whittaker, D. M. Strong Exciton-Photon Coupling in an Organic Semiconductor Microcavity. *Nature* **1998**, *395*, 53–55.
14. Bonnand, C.; Bellessa, J.; Plenet, J. C. Properties of Surface Plasmons Strongly Coupled to Excitons in an Organic Semiconductor Near a Metallic Surface. *Phys. Rev. B* **2006**, *73*, 245330.
15. Gouterman, M. Spectra of Porphyrins. *J. Mol. Spectrosc.* **1961**, *6*, 138.
16. Berrier, A.; Offermans, P.; Cools, R.; van Megen, B.; Knoben, W.; Vecchi, G.; Gómez Rivas, J.; Crego-Calama, M.; Brongersma, S. H. Enhancing the Gas Sensitivity of Surface Plasmon Resonances with a Nanoporous Silica Matrix. *Sensor Actuat. B: Chem.* **2011**, in press, doi: 10.1016/j.snb.2011.07.030.
17. Jahnke, F.; Kira, M.; Koch, S. W.; Khitrova, G.; Lindmark, E. K.; Nelson, T. R., Jr.; Wick, D. V.; Berger, J. D.; Lyngnes, O.; Gibbs, H. M. Excitonic Nonlinearities of Semiconductor Microcavities in the Nonperturbative Regime. *Phys. Rev. Lett.* **1996**, *77*, 5257–5260.
18. Homola, J.; Yee, S. S.; Gauglitz, G. Surface Plasmon Resonance Sensors: Review. *Sensor Actuat. B: Chem.* **1999**, *54*, 3–15.
19. Salomon, A.; Genet, C.; Ebbesen, T. W. Molecule−Light Complex: Dynamics of Hybrid Molecule−Surface Plasmon States. *Angew. Chem. Int. Ed.* **2009**, *48*, 8748–8751.
20. Tischler, J. R.; Bradley, M. S.; Zhang, Q.; Atay, T.; Nurmikko, A.; Bulovic, V. Solid State Cavity QED: Strong Coupling in Organic Thin Films. *Org. Electron.* **2007**, *8*, 94–113.
21. Kumar, G. A.; Thomas, V.; Jose, G.; Unnikrishnan, N. V.; Nampoori, V. P. N. Optical Properties of Porphyrins in Borate Glassy Matrix. *Mater. Chem. Phys.* **2002**, *73*, 206–211.
22. Tillekaratne, A. D.; de Silva, R. M.; Nalin de Silva, K. M. Push Pull Porphyrins as Non-linear Optical Materials: Ab initio Quantum Chemical Calculations. *J. Mol. Struct.* **2003**, *638*, 169–176.
23. Maex, K.; Baklanov, M. R.; Shamiryan, D.; Iacopi, F.; Brongersma, S. H.; Yanovitskaya, Z. S. Low Dielectric Constant Materials for Microelectronics. *J. Appl. Phys.* **2003**, *93*, 8793–8841.
24. Dolphin, D. *The Porphyrins*; Academic Press: New York, 1978.
25. O'Neil, M. P.; Niemczyk, M. P.; Svec, W. A.; Gosztola, D.; Gaines, G. L., III; Wasielewski, M. R. Picosecond Optical Switching Based on Biphotonic Excitation of an Electron Donor Acceptor-Donor Molecule. *Science* **1992**, *257*, 63–65.
26. Lin, V. S.-Y.; DiMagno, S. G.; Therien, M. J. Highly Conjugated Acetylenyl Bridged Porphyrins: New Models for Light-Harvesting Antenna Systems. *Science* **1994**, *264*, 1105–1111.
27. Wright, J. D.; Cado, A.; Peacock, S. J.; Rivalle, V.; Smith, A. M. Effects of Nitrogen Dioxide on Surface Plasmon Resonance of Substituted Phtalocyanine Films. *Sensor Actuat. B: Chem.* **1995**, *29*, 108–114.
28. Mc Naughton, A. J.; Richardson, T. H.; Barford, W.; Dunbar, A.; Hutchinson, J.; Hunter, C. A. Characterisation of the Reaction of Free-base Porphyrins to Nitrogen Dioxide. *Colloid Surf. A* **2006**, *284*, 345–349.